




Sorting of heterogeneous colloids by AC-dielectrophoretic forces in a microfluidic chip with asymmetric orifices

Journal Article

Author(s):

Zhao, Kai; [Hu, Minghan](#) ; [van Baalen, Carolina](#) ; Alvarez, Laura; [Isa, Lucio](#) 

Publication date:

2023-03-15

Permanent link:

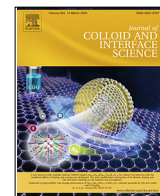
<https://doi.org/https://doi.org/10.3929/ethz-b-000589657>

Rights / license:

[Creative Commons Attribution 4.0 International](#)

Originally published in:

Journal of Colloid and Interface Science 634, <https://doi.org/10.1016/j.jcis.2022.12.108>



Sorting of heterogeneous colloids by AC-dielectrophoretic forces in a microfluidic chip with asymmetric orifices

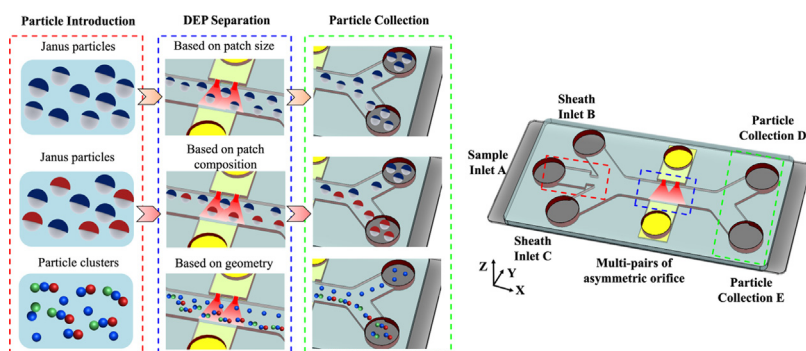


Kai Zhao^{a,b,*}, Minghan Hu^b, Carolina van Baalen^b, Laura Alvarez^b, Lucio Isa^{b,*}

^a Liaoning Key Laboratory of Marine Sensing and Intelligent Detection, Department of Information Science and Technology, Dalian Maritime University, 116026 Dalian, China

^b Laboratory for Soft Materials and Interfaces, Department of Materials, ETH Zurich, 8093 Zurich, Switzerland

GRAPHICAL ABSTRACT



ARTICLE INFO

Article history:

Received 14 September 2022

Revised 12 December 2022

Accepted 19 December 2022

Available online 21 December 2022

Keywords:

AC dielectrophoresis

Janus particles

Patchy particles

Particle clusters

Sorting and manipulation

ABSTRACT

Hypothesis: The synthesis of compositionally heterogeneous particles is central to the development of complex colloidal units for self-assembly and self-propulsion. Yet, as the complexity of particles grows, synthesis becomes more prone to “errors”. We hypothesize that alternating-current dielectrophoretic forces can efficiently sort Janus particles, as a function of patch size and material, and colloidal dumbbells by size.

Experiments: We prepared Janus particles with different patch size and material by physical vapor deposition and colloidal dumbbells via capillarity-assisted particle assembly. We then performed sorting experiments in a microfluidic chip comprising electrodes with asymmetric orifices, specifically exploiting the dielectric contrast between different portions of the particles or their size difference to steer them towards different outlets.

Findings: We calculated that the DEP force for Janus particles may switch from positive to negative as a function of composition at a critical AC frequency, thus enabling sorting different particles crossing the electrodes’ region. The predictions are confirmed by optical microscopy experiments. We also show that intact and “broken” dumbbells can be simply separated as they experience different DEP forces. The integration of multiple asymmetric orifices leads a larger zone with high field gradient to increase separation efficiency and makes it a promising tool to select precise particle populations, isolating fractions with narrowly distributed characteristics.

© 2022 The Authors. Published by Elsevier Inc. This is an open access article under the CC BY license (<http://creativecommons.org/licenses/by/4.0/>).

* Corresponding authors.

E-mail addresses: kai.zhao@dlmu.edu.cn (K. Zhao), lucio.isa@mat.ethz.ch (L. Isa).

1. Introduction

The development of colloidal particles presenting a complex structure and an inhomogeneous composition has been a target of the soft matter community over the past few decades [1,2]. Moving away from uniform spherical particles with isotropic properties and interactions, i.e. by breaking their compositional symmetry, enables directionality, an essential feature required for the emergence of complex structures, e.g. via self-assembly [3,4], and of new physical behavior, e.g. self-propulsion [5].

Among complex anisotropic particles, spherical Janus particles, which display two regions with different physical or chemical properties (such as charge, hydrophobicity and surface chemistry) arguably are the simplest class of compositionally asymmetric colloids [6]. In spite of the apparent simplicity, this asymmetry is at the basis of their importance and potential for a broad range of applications and research directions [7], including drug delivery [8–10], microrobotics [11], lab-on-a-chip assays [12], and biomedical applications [3]. However, many of the features of the final materials and of their applications strongly depend on small variations of the patch characteristics. As an example, from a fundamental viewpoint, colloids exhibiting attractive patches undergo a fluid–fluid phase separation that strongly depends on the patch size [13], and small variations in the patch size enable the self-assembly of different structures [14]. Similarly, in applications, the ratio between the two surface patches strongly affects the adsorption of Janus particles at water–oil interfaces [15] and thus their ability to stabilize different kinds of Pickering emulsions [16]. Concerning self-propulsion, inhomogeneity of the cap morphology has been shown to strongly affect particle trajectories. [17] As a next step, one of the possible routes to increase compositional and geometrical complexity is to produce clusters of different spherical particles in prescribed arrangements, a system often referred to as “colloidal molecules” [18]. However, achieving an *a priori* control on the particle properties is an elusive task and, typically, a statistical distribution of colloidal molecules with different number or positions of “atoms” is obtained, which need to be sorted *a posteriori* [19,20].

An opportunity to address this challenge may come from microfluidic systems and platforms, which have been widely utilized for the manipulation of micro and nanoscale objects [21]. Among various options, dielectrophoresis (DEP) is a reliable approach to provide accurate manipulation of targeted particles [22–24]. DEP forces induce the movement of dielectric particles owing to the polarization effects between the particles and the suspending medium in a non-uniform electric field [25–27]. Generally, an alternating current (AC) inhomogeneous electric field can be generated via an array of micro-electrodes with patterned configurations, which are embedded in a microchannel [28,29], while inhomogeneous direct current (DC) electric fields are typically obtained by larger external electrodes in the presence of patterns of insulating obstacles within the channel [30–32]. Since the magnitude and direction of the dielectrophoretic forces rely on the particles' size and dielectric properties, which depend on their morphology and composition, DEP enables selective and sensitive particle analysis [33–35].

In this work, we design an AC-DEP microfluidic chip containing multiple asymmetric orifices for the sorting of Janus colloids with desired patch size and material and for the separation of intact and broken polystyrene dumbbells produced by sequential capillary assembly. The presence of multiple orifices increases the size of the separation region, leading to the effective sorting of the target particles within our microfluidic chip.

2. Materials and methods

2.1. AC dielectrophoresis

The general formulation for the DEP force exerting on the spherical particle is given by [36]

$$F_{DEP} = 2\pi\epsilon_m r^3 \text{Re}(f_{CM}) (\nabla|E|^2) \quad (1)$$

where r describes the particle radius, ϵ_m is the dielectric constant of the suspending medium, $\nabla|E|^2$ represents the electric field gradient, and $\text{Re}(f_{CM})$ is the real part of the complex Clausius-Mossotti factor (f_{CM}), describing the relative polarizabilities of the particles and the medium. We first provide an application of this general expression to the case of a Janus particle, such as the one represented in Fig. 1, and then comment on its relevance for dumbbell separation.

The dielectrophoretic motion of the Janus particle results from the sum of the DEP forces on the volumes corresponding to the coated (Core-Patch) and the uncoated (Core) parts of the colloid and, as previously derived in [25,37–39], is given by

$$F_{DEP,Janus} = 2\pi\epsilon_m r^3 [K\text{Re}(f_{CM,Core}) + (1-K)\text{Re}(f_{CM,Core-Patch})] (\nabla|E|^2) \quad (2)$$

where K is the volume fraction of the uncoated part of the Janus colloid which, in the limit of thin coatings ($r_1 \ll r$), is related to the patch area T as

$$K = 3(1-T)^2 \left(1 - \frac{2(1-T)}{3}\right) \quad (3)$$

Comparing Eq (1) and (2), we can recover the generic form of the DEP force for the whole Janus particle by defining an effective CM factor as

$$\text{Re}(f_{CM,Janus}) = K\text{Re}(f_{CM,Core}) + (1-K)\text{Re}(f_{CM,Core-Patch}) \quad (4)$$

where the CM factor for the uncoated, core sphere is written as

$$f_{CM,Core} = \left(\frac{\epsilon_{Core}^* - \epsilon_m^*}{\epsilon_{Core}^* + 2\epsilon_m^*}\right) \quad (5)$$

The CM factor for the coated sphere is expressed by a shell model [40]:

$$f_{CM,Core-Patch} = \left(\frac{\epsilon_{Core-Patch}^* - \epsilon_m^*}{\epsilon_{Core-Patch}^* + 2\epsilon_m^*}\right) \quad (6)$$

$$\epsilon_{Core-Patch}^* = \epsilon_{Patch}^* \left[\gamma_{12}^3 + 2\left(\frac{\epsilon_{Core}^* - \epsilon_{Patch}^*}{\epsilon_{Core}^* + \epsilon_{Patch}^*}\right) \right] / \left[\gamma_{12}^3 - \left(\frac{\epsilon_{Core}^* - \epsilon_{Patch}^*}{\epsilon_{Core}^* + \epsilon_{Patch}^*}\right) \right] \quad (7)$$

where $\epsilon^* = \epsilon - (j\sigma/\omega)$ represents the complex permittivity, ϵ and σ are the dielectric constant and electrical conductivity, respectively. The particles' electrical conductivity can be expressed by $\sigma = \sigma_b + 2K_s/r$. The bulk conductivity σ_b can be neglected and the surface conductance K_s is taken as 1 nS for polystyrene particles [41–43]. The angular frequency of the electric fields is described as $\omega = 2\pi f$ and $j = \sqrt{-1}$. Finally, the factor γ_{12} accounts for the relative coating thickness and is defined as $\gamma_{12} = (r + r_1)/r$. In the case of the Janus particles, if $\text{Re}(f_{CM,Janus}) < 0$, the DEP force is negative and will repel the Janus particles away from the regions of high electric field. While, if $\text{Re}(f_{CM,Janus}) > 0$, the colloids will be attracted towards areas of high electric fields and the force is said to be positive. Since the sign of $\text{Re}(f_{CM,Janus})$ may depend on frequency, for a given set of materials and patch geometries, an inversion of the direction of the DEP force can be achieved by adjusting the frequency of the electric field, and thus selectively steering the Janus particles with desired patch properties in a prescribed region of

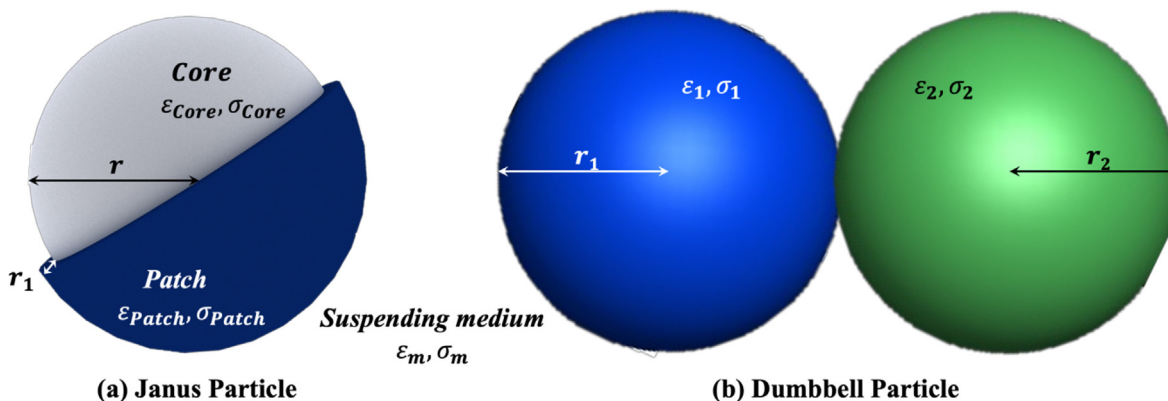


Fig. 1. Left: Schematic illustration of a Janus particle with a hemispherical patch. Right: Schematic illustration of a dumbbell particle.

the microfluidic chip. The use of AC-DEP therefore presents additional advantages relative to DC-DEP [31,32] in that the force acting on the particles can be dynamically adjusted during the experiment.

Moreover, as it can be seen in Eq (1), the magnitude of the DEP force is proportional to the volume of the particles (r^3). Therefore, as the deviation of particle trajectory is proportional to the magnitude of the DEP forces acting on them, particles of different diameters will flow into different streamlines after moving through the inhomogeneous electric field area and can be collected in different outlet channels. As a simple case, a compositionally homogeneous and symmetric dumbbell will experience a force double the one experienced by each individual lobe. Since in this case the direction of the force has the same frequency dependence for both dumbbells and individual particles, the only handle available to increase sorting efficiency is to achieve a higher gradient of the electric field over a greater area, as we reach with our multiple asymmetric orifices. Conversely, in the case of compositionally heterogeneous dumbbells, the direction of the force depends on the total sign of $Re(f_{CM})$, and two different types of particles may have opposite DEP behaviors. The same concept can be extended to clusters comprising a larger number of particles.

2.2. Preparation of Janus particles and dumbbells

The Janus colloids used in our experiments were prepared starting from sulfate polystyrene particles (microParticles, GmHH) of 4.5 μm diameter as cores. We first assembled monolayers of the polystyrene particles drying a 200 μL droplet of a diluted suspension (0.35 %w/v) on a pre-cleaned microscope slide. Platinum and silica are then sputter-coated onto the monolayer with the application of glancing angle deposition method (GLAD) [11,44] to produce the surface patches (E-beam Evaporator-Plassys MEB550S, FIRST Clean Room). In order to achieve different surface areas of the coating patch, various incidence angles were applied, i.e. 10°, 20°, 45°, 90°, approximately corresponding to surface areas T of 10%, 20%, 35%, and 50%, respectively [44] (Figure S-1). We deposited platinum and silica caps with thickness of 50 nm, 75 nm, and 100 nm to examine the effect of coating thickness. Finally, after coating, the particles were released from the substrate into MilliQ water via ultra-sonication [45].

Colloidal dumbbells were fabricated from sulfonated polystyrene spheres with a diameter of 2.80 μm polystyrene microparticles (PS-FluoGreen-Fi135, MicroParticles, GmHH) using sequential Capillarity-Assisted Particle Assembly (sCAPA) [46–48]. In brief, an aqueous particle suspension containing 0.05 % Triton X-100 (Sigma-Aldrich), 0.5 mM SDS (Sigma-Aldrich), and 1 mg/mL particles was made. A 55 μL droplet of the parti-

cle suspension was dragged over a 0.5x1 cm^2 PDMS slab containing 2200 traps of 1.4x6.2x3 μm^3 (HxLxW) with a speed of 4 $\mu\text{m/s}$. After depositing the first particle, a second droplet of particle suspension was dragged over the traps to deposit the second particle. The resulting particle pairs were sintered for 15 min. at 75 °C, yielding mostly dumbbells, but also single particles from partially filled traps. From microscopy images, an average yield of 78 % dumbbells and 22 % individual particles was calculated.

2.3. Fabrication of a microfluidic chip with multiple asymmetric orifices

The fabrication of the AC-DEP microfluidic chip for the sorting of Janus particles follows a traditional soft lithography method [49]. Briefly, a master with raised features is fabricated and replicated in PDMS. The PDMS layer is permanently bonded to the substrate after plasma treatment. The copper electrode pads with patterned geometry (Sigma-Aldrich) are created by spin-coating a thick SU-8 photoresist (MicroChem) layer on the electrode pad, submerging it in the photoresist developer and dissolving the uncross-linked photoresist after UV treatment. Following that, the fabrication process of the micro-copper-electrodes, whose thickness and width are 25 μm and 500 μm , respectively, is schematically described in Figure S-2. Then the micro-copper-electrodes are firmly embedded in the deformable microchannel. By adjusting the suspension levels in the reservoirs of the micro-electrode chambers (yellow circular pads in Fig. 2), the liquid leakage through the gaps can be neglected [30]. The final chip is represented in Fig. 2, including a triple inlet branch and the main channel with two outlet branches. The height of the whole channel is uniformly 27 μm . The main channel has a width of 200 μm and 500 μm in length. The sample inlet A, outlets D and E are 100 μm in width, and the sheath flow inlets B and C have a width of 200 μm , respectively. In particular, two pairs of asymmetric orifices, comprising two 10 μm -wide small orifices, separated by 50 μm , and a 500 μm -wide large orifice on the opposite side of the microchannel, are situated in the main horizontal section of the chip. The Janus colloids and the dumbbells are introduced into the sample inlet branch A and driven along the horizontal microchannel by liquid pressure (i.e., controlled by the liquid height difference between the inlets and outlets wells). Then, focused by the sheath flow from the inlet branches B and C, they flow along the centered streamlines through the AC-DEP region and across the two asymmetric-orifice pairs. Ultimately, the particles migrate into different outlet collection channels, accordingly to the DEP forces they experience.

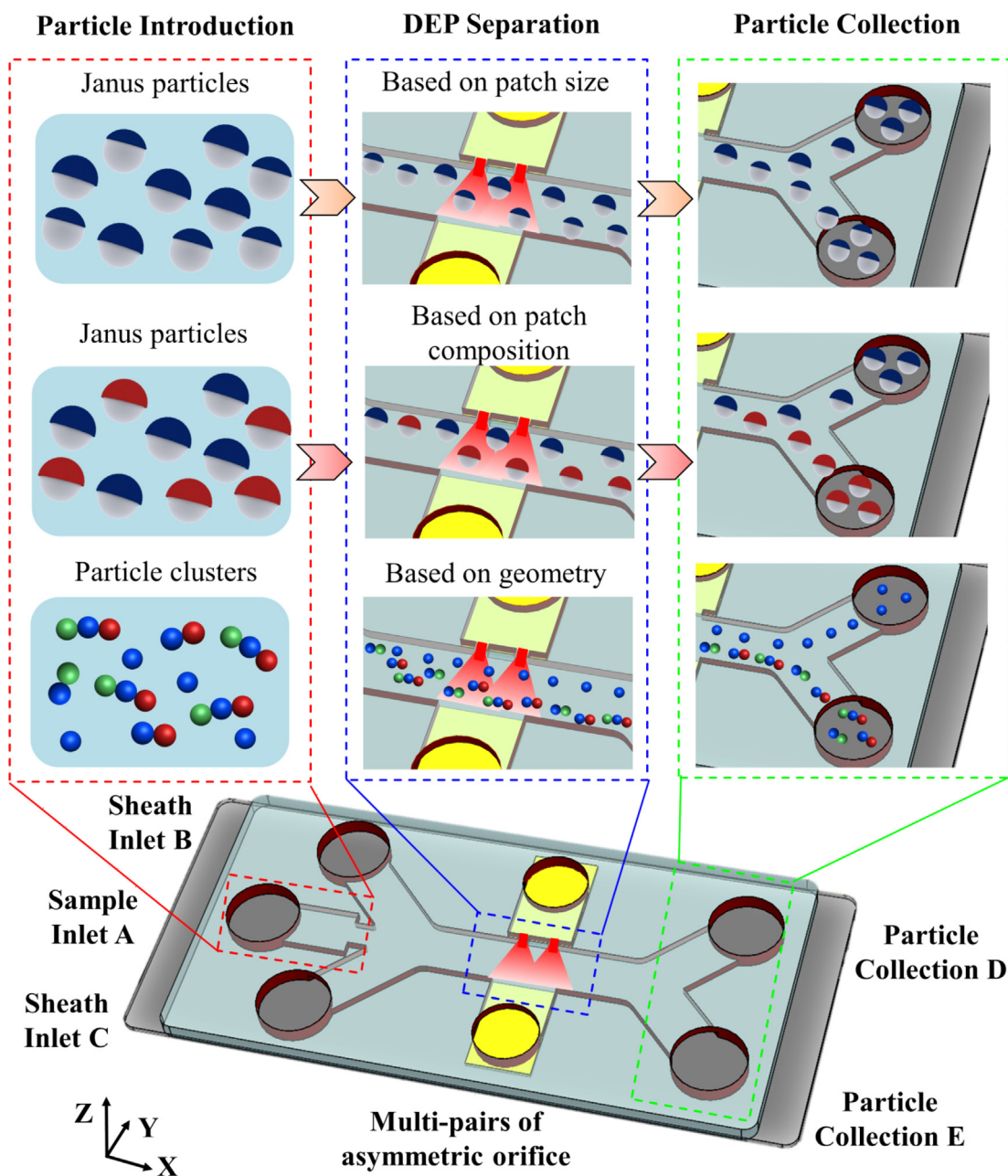


Fig. 2. Schematic of the AC-DEP microfluidic chip with two pairs of asymmetric orifices for the sorting of Janus particles based on patch area and patch composition, and particle clusters based on size. The yellow circular pads are utilized for the connection of the electrodes to the function generator. The inlets and outlets for the fluidic channels are connected to tubing for sample insertion and collection. This figure shows the side view of the microchannel and is not drawn to scale. (For interpretation of the references to colour in this figure legend, the reader is referred to the web version of this article.)

2.4. Experimental setup

The AC-DEP sorting experiments are started by introducing the DI water into the microchannel, and then 10 μL of the particles solution and the surrounding solution is loaded into reservoirs A, B, and C, respectively. The particles transport in the microchannel is driven by the liquid level between the inlet and outlet reservoirs and the flow rate is approximately $1.35 \times 10^{-3} \mu\text{L/s}$. The velocity and the residence time of the particles passing through the microelectrodes, i.e., the DEP effective area, are approximately 250 $\mu\text{m/s}$ and two seconds, respectively. To generate the gradient of the electric field, i.e., the DEP forces, a square wave AC electric field of tunable amplitude and frequency is applied to the microelectrodes using a function generator (Agilent 33522A, up to 10 MHz and

10 Vpp). When passing near the small orifices, the particles experience the strongest electric field gradient and are either drawn towards it by the positive AC-DEP effects or repelled away from it by the negative AC-DEP effects (schematically shown in Fig. 2). In particular, by using asymmetric orifices with a large width ratio and a short length of the small orifice, a stronger electric field gradient and hence stronger DEP forces can be produced, resulting in high-resolution sorting (shown in Figure S-3). The separation resolution can be further enhanced by utilizing sequential pairs of asymmetric orifices, as demonstrated later by numerical simulations (COMSOL 5.4) and implemented in the experiments (Figure S-3). Furthermore, in our design, the electrodes generate the inhomogeneous electric fields without changing the cross-section of the horizontal channel, and the field gradient, which is

orthogonal to the flow direction, has no influence on particle transport along the channel, which is pressure-controlled. The sorting of the particles is monitored in an inverted microscope fitted with a high-speed CCD camera and a fluorescence source (Eclipse Ti2-E, Nikon). To analyze the sorting efficiency, approximately thirty particles in a minute are counted to flow into the respective collection channel. The colloids are characterized via scanning electron microscopy (SEM). Finally, the sorting efficiency is estimated by counting the number of particles flowing into each outlet channel during the experiments.

3. Results and discussion

3.1. Effect of patch area on the sorting of Janus particles

We start by examining the effects of the patch surface areas on the DEP behavior of the Pt-coated Janus particles varying with the applied AC electric field frequency. As indicated by Eq. (4), the values of the CM factor determine the sign of the DEP forces on the Janus particles. The values of the parameters used for calculating the CM factors of the Janus particles are shown in Table S-1, and the results of the calculations are reported in Fig. 3.

At low frequency ($<10^4$ Hz), all particles show a positive DEP, irrespective of the patch size. As the frequency increases, $Re(f_{CM,Janus})$ decreases towards the high-frequency plateau. However, this latter plateau value depends on the surface coverage of the Pt patch and for a patch area \sim (and smaller) 35 %, it actually becomes negative. Therefore, there is a critical frequency between 10^5 and 10^6 Hz for which the sign of the DEP force is inverted. Moreover, this critical frequency is patch size-dependent, so that the sign inversion is experienced first by particles with a smaller patch and then by particles with larger patches. This response allows us to tune the applied frequency so that it is greater than the critical frequency only for patch sizes below a target value and thus to separate those particles from the rest.

The selectivity of the sign of the DEP force allows, for instance, not just the sorting of pure PS particles from Janus ones, but also to separate particles with 50 % coverage from ones with 35 % coverage, as shown in Fig. 4. In fact, at 1 MHz, the values of $Re(f_{CM,Janus})$ for Janus particles with no platinum patch (i.e., homogeneous polystyrene particles), a 35 % platinum patch area, and a

50 % platinum hemisphere are -0.467 , -0.054 , and 0.266 , respectively. Fig. 4(a) shows that a mixed sample of homogeneous polystyrene particles and Janus particles with 50 % platinum hemisphere is injected in the microfluidic channel and when the particles cross the electrode region, the homogeneous (non-fluorescent) colloids are pushed away by the negative DEP forces to flow towards the negative DEP collection. Conversely, the Janus particles with a 50 % platinum patch (fluorescent) are attracted by the positive DEP forces away from the large orifice and flow into the positive DEP collection. A similar behavior is observed in Fig. 4(b), where a mixture of Janus particles with 35 % platinum surface coverage (non-fluorescent) and 50 % platinum surface coverage (fluorescent) are sorted and move into the negative and positive DEP collection channels, respectively (see Supplementary Movie S1). Under these conditions, 100 % of the $4.5 \mu\text{m}$ polystyrene Janus particles with 50 % coating move into the positive DEP collection channel D. Conversely, 91 % of the particles with a patch area of 35 % go into the negative DEP collection channel E and the remaining 9 % ends up being collected in the wrong outlet. This partially imperfect sorting derives from the fact that, given the differences in the absolute values of $Re(f_{CM,Janus})$, the DEP force acting on the Janus particles with 35 % coverage is smaller than the one acting on the particles with 50 % coverage. Therefore, occasionally, the vertical displacement induced by the negative DEP force is not sufficient to push the 35 % Janus particles into the right collection outlet. This situation can happen any time there is a large difference in the absolute values of $Re(f_{CM,Janus})$ between the particles to be sorted and can be resolved by increasing the area of high field gradient, such that the corresponding displacements are larger. **Supplementary Movie S1.**

3.2. Effect of patch material on the sorting of Janus particles

After demonstrating the possibility to sort particles by patch size, we also show that our AC-DEP-based approach enables sorting particles with different composition. As an example, we choose $4.5 \mu\text{m}$ polystyrene Janus particles with 50 % coverage of Pt and silica, respectively. Fig. 5 shows that the frequency response of the

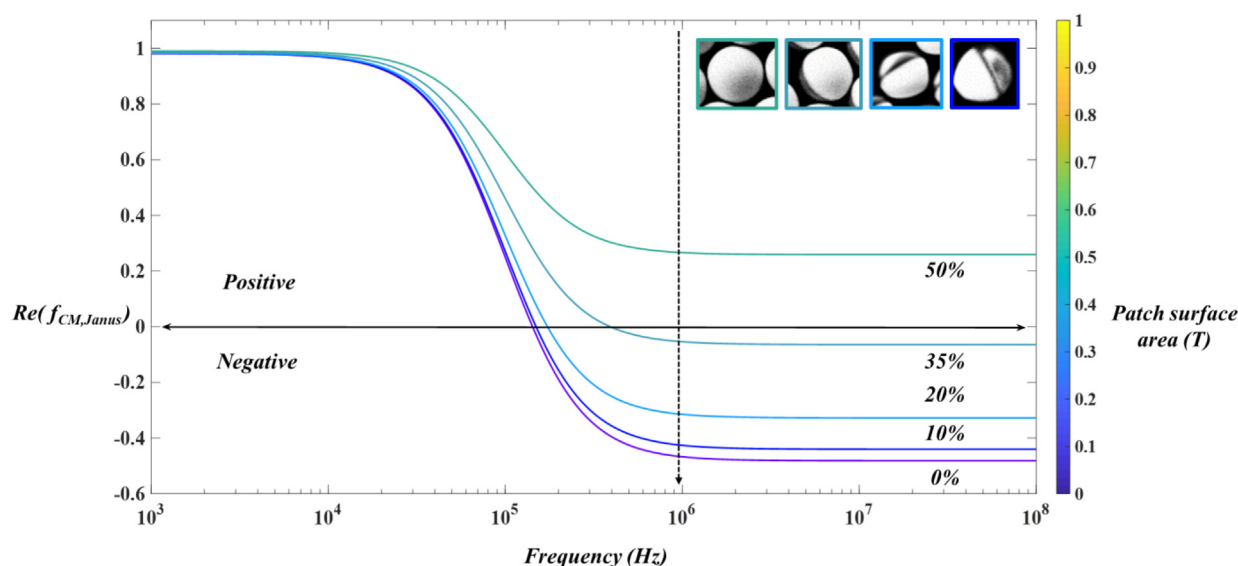


Fig. 3. Calculated real part of $f_{CM,Janus}$ as a function of applied AC field frequency for the $4.5 \mu\text{m}$ polystyrene Janus particles with five different platinum patch surface areas: 0 %, 10 %, 20 %, 35 %, 50 %, colored according to the scale bar. The thickness of the platinum patch is 100 nm.

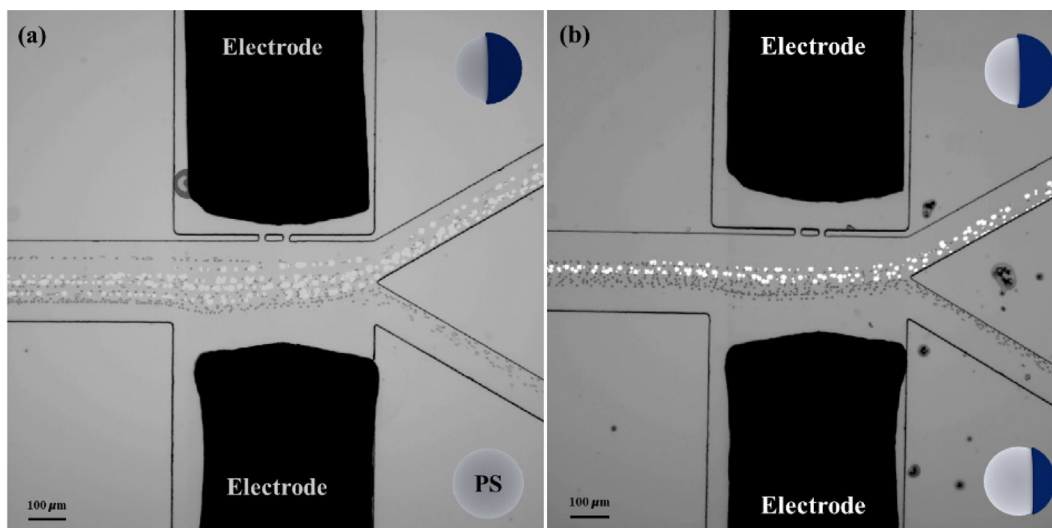


Fig. 4. Long-exposure micrographs showing: (a) the separation of 4.5 μm polystyrene Janus particles with a platinum hemisphere (P-DEP, fluorescent) and uncoated polystyrene particles (N-DEP, non-fluorescent). (b) the separation of 4.5 μm polystyrene Janus particles with a platinum hemisphere (P-DEP, fluorescent) and Janus particles with platinum patch size of 35 % (N-DEP, non-fluorescent). The thickness of the platinum patch is 100 nm. The applied V_{pp} is 10 V and frequency is 1 MHz.

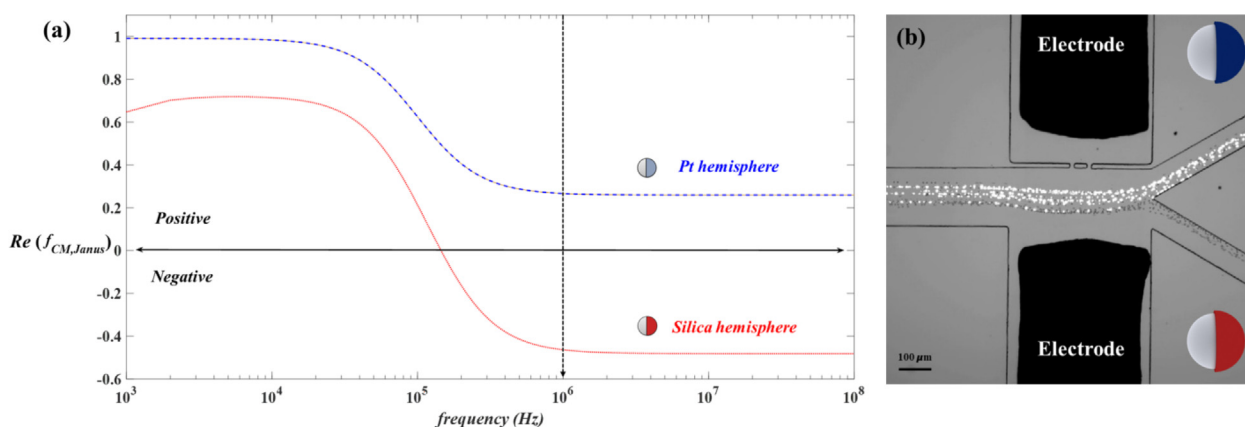


Fig. 5. (a) Calculated real part of $f_{CM,Janus}$ as a function of applied AC field frequency for the 4.5 μm polystyrene Janus particles with a platinum and a silica hemisphere. The patch thickness is 100 nm. (b) Long-exposure micrographs showing the separation of 4.5 μm polystyrene Janus particles with a platinum hemisphere (P-DEP, fluorescent) and a silica hemisphere (N-DEP, non-fluorescent). The thickness of the platinum and silica patch is 100 nm. The applied V_{pp} is 10 V and frequency is 1 MHz.

polarizability is different for the two materials, with the real part of the CM factors changing sign for the silica-coated particles at $\sim 10^5$ Hz, while the corresponding quantity for the Pt-coated particles remains always positive.

As shown in Fig. 5, at 1 MHz, the Janus particles with the platinum hemisphere ($Re(f_{CM,Janus}) \approx 0.266$, fluorescent) experience a positive DEP force and flow into the corresponding collection channel, and 100 % of them move into the positive DEP collection channel D. Conversely, at the same frequency, the Janus particles with silica hemisphere ($Re(f_{CM,Janus}) \approx -0.463$, non-fluorescent) experience a negative DEP force and are pushed away from the small orifice region, while, 87 % of them go into the negative DEP collection channel E.

3.3. Effect of patch thickness on the trajectory of Janus particles

Finally, we show that the thickness of the metallic cap has no discernible effect in terms of the DEP force, and thus that the method cannot be used to sort particles with broadly distributed coating thickness. In particular, we compute the $Re(f_{CM,Janus})$ for 4.5 μm polystyrene-based Janus particles with a platinum hemispherical cap and thickness of 50 nm, 75 nm, and 100 nm, respectively, varying

with the applied AC electric field frequency. Going back to the definition reported in Equation (7), the factor γ_{12} accounts for the relative coating thickness and is defined as $\gamma_{12} = (r + r_1)/r$. Therefore, in the limit of thin coatings ($r_1 \ll r$), variations in γ_{12} becomes negligible and then the thickness of the metallic cap shows no discernible effect in terms of the DEP force. From Figure S-4, we observe that the $Re(f_{CM,Janus})$ values for Janus particles with different hemisphere thickness essentially overlap across the whole frequency spectrum. Therefore, we expect those Janus particles to undergo similar DEP effects and move into the same outlet collection. As shown in Figure S-5, for three different frequencies of the AC electric fields, i.e., 1 kHz, 100 kHz, and 1 MHz, a mixture of the Janus particles with hemisphere thickness of 50 nm, 75 nm, and 100 nm always shows a positive DEP behavior and all particles move together into the upward outlet collection channel, proving that patch thickness does not affect their motion.

3.4. Isolation of dumbbells

We conclude by showing that our setup enables the efficient separation of polystyrene dumbbells from individual spheres, which result from the incomplete yield of the sCAPA deposition

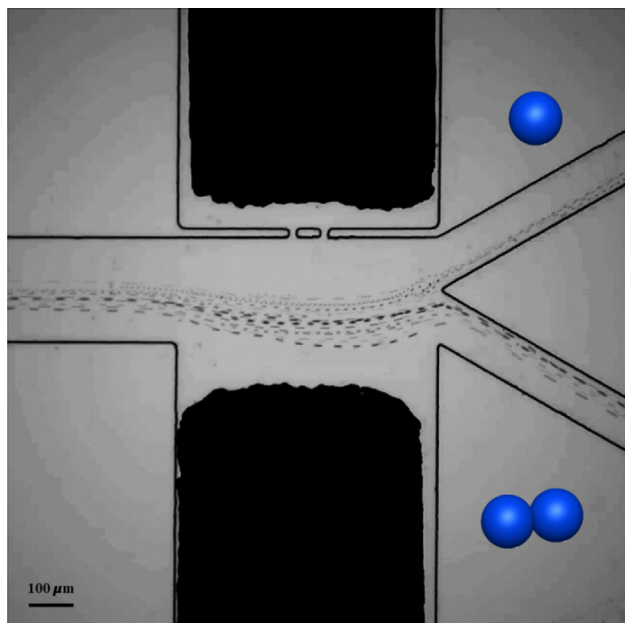


Fig. 6. Long-exposure micrographs showing the separation of individual 2.8 μm polystyrene particles and dumbbells consisting of two of the same polystyrene particles. The applied V_{pp} is 10 V and frequency is 1 MHz (All these microparticles experience negative DEP effects, but of different magnitude).

or that break off during harvesting and redispersion. As previously mentioned, the value of the DEP force is proportional to the particle volume, leading to a straightforward separation of particle clusters based on their size. In particular, the magnitude of the DEP forces acting on the dumbbells is approximately twice that acting on the single polystyrene particles. As shown in Fig. 6, the stronger DEP force in the multiple asymmetric orifice area causes greater trajectory changes for the dumbbells (appearing as darker spots the long-exposure image), leading to significantly different trajectories of the individual particles and the dumbbells. Consequently, they are deflected into distinct outlet channels. Single particles undergo relatively weaker AC-DEP forces and 93 % of them move into the upper outlet collection D, while the dumbbells undergo stronger AC-DEP forces and 92 % of them flow into the lower outlet collection E (see Supplementary Movie S2). **Supplementary Movie S2.**

4. Conclusions

Among the broad range of available separation techniques, a microfluidic AC-DEP approach presents significant advantages in terms of selectivity and integration with experimental platforms for the manipulation and assembly of various Janus particles and micro/nano particles [22,28,39,50–55]. By inducing an inhomogeneous electric field across the microchannel via two pairs of asymmetric orifices, i.e. consisting of multiple small orifices and a large orifice on the opposite sidewalls in the horizontal channel, the DEP effective region is enlarged and the time period of DEP forces acting on the particles is extended. In this way, the trajectory difference between different particles passing through the vicinity of the small orifices is increased, and we show that stronger AC-DEP effects are experienced by the particles, leading to higher sorting efficiency and resolution. While the previously reported average sorting efficiency for particles, droplets and cells [26,31,32,56,57] was approximately 89 % with a single pair of

asymmetric orifices, using two pairs enabled us to push it to 94 %. By tuning the applied frequency of the AC electric field, the direction of the AC-DEP forces switches from positive to negative at a particle-dependent critical frequency, and the magnitude of the AC-DEP forces scales linearly with the particle volume, resulting in the successful sorting of different particles by composition and size with an average sorting efficiency as high as 90 %. In particular, selecting Janus particles with a specific patch size is of high relevance in a wide range of applications, including drug delivery, autonomously powered microgears and microrobotics, environmental remediation, flow generation, separation technology, and lab-on-chip assays [58,59,68,60–67]. Moreover, the ability of separating mixed particle populations by adjusting the AC frequency on chip identifies this method as a promising technique to precisely select particles in complex colloids and remove undesired particles from a target suspension. This latter aspect is particularly interesting in conjunction with synthesis strategies for complex colloids such as emulsion templating, stimulated dewetting, colloidal fusion, swelling and aggregation or capillarity-assisted particle assembly [20,41,47,69,70]. In all these methods, mixed particle populations are produced, with a sub-100 % yield of the target particles requiring post-synthesis sorting to achieve a completely uniform population, as desirable for studies on self-assembly or self-propulsion [46,71,72]. We thus envisage the future integration of our device into microfluidic chips, where an as-synthesized ensemble of complex colloids (also with the potential for on-chip synthesis [73,74]), can be sorted to select a sub-population of particles with narrowly distributed properties. These particles can be directed to another region of the same chip where additional experiments can be carried out, thus enabling a robust, streamlined approach to study monodisperse fractions of complex colloids under controlled conditions.

CRediT authorship contribution statement

Kai Zhao: Conceptualization, Formal analysis, Funding acquisition, Methodology, Software, Visualization, Writing – original draft, Writing – review & editing. **Minghan Hu:** Resources, Writing – review & editing. **Carolina van Baalen:** Resources, Writing – review & editing. **Laura Alvarez:** Resources, Writing – review & editing. **Lucio Isa:** Conceptualization, Formal analysis, Funding acquisition, Methodology, Project administration, Supervision, Writing – original draft, Writing – review & editing.

Data availability

Data will be made available on request.

Declaration of Competing Interest

The authors declare that they have no known competing financial interests or personal relationships that could have appeared to influence the work reported in this paper.

Acknowledgements

This work is supported by China Postdoctoral Science Foundation (Grant No. 2021M690500), Fundamental Research Funds for the Central Universities of China (Grant No. 3132022247), Natural Science Foundation of Liaoning Province (2022-BS-100), Startup Research Foundation for Talents of Dalian Maritime University (Grant No. 02500352) and the MCSA-ITN-ETN “ActiveMatter” Grant agreement No.812780.

References

- [1] W. Li, H. Palis, R. Merindol, J. Majimel, S. Ravaine, E. Duguet, Colloidal molecules and patchy particles complementary concepts, synthesis and self-assembly, *Chem. Soc. Rev.* 49 (2020) 1955–1976, <https://doi.org/10.1039/C9CS00804G>.
- [2] A.B. Pawar, I. Kretzschmar, Fabrication, assembly, and application of patchy particles, *Macromol. Rapid Commun.* 31 (2010) 150–168, <https://doi.org/10.1002/marc.200900614>.
- [3] J.R. Millman, K.H. Bhatt, B.G. Prevo, O.D. Velev, Anisotropic particle synthesis in dielectrophoretically controlled microdroplet reactors, *Nat. Mater.* 4 (2005) 98–102, <https://doi.org/10.1038/nmat1270>.
- [4] J. Zhang, E. Luijten, S. Granick, Toward design rules of directional janus colloidal assembly, *Annu. Rev. Phys. Chem.* 66 (2015) 581–600, <https://doi.org/10.1146/annurev-physchem-040214-121241>.
- [5] C. Bechinger, R. Di Leonardo, H. Lowen, C. Reichhardt, G. Volpe, G. Volpe, Active particles in complex and crowded environments, *Rev. Mod. Phys.* 88 (2016), <https://doi.org/10.1103/RevModPhys.88.045006>.
- [6] A. Walther, A.H.E. Mu, Janus particles: synthesis, self-assembly, physical properties, and applications, *Chem. Rev.* (2012).
- [7] J. Zhang, B.A. Grzybowski, S. Granick, Janus particle synthesis, assembly, and application, *Langmuir.* 33 (2017) 6964–6977, <https://doi.org/10.1021/acs.langmuir.7b01123>.
- [8] S. Sundararajan, P.E. Lammert, A.W. Zudans, V.H. Crespi, A. Sen, Catalytic motors for transport of colloidal cargo, *Nano Lett.* 8 (2008) 1271–1276, <https://doi.org/10.1021/nl072275j>.
- [9] A.M. Boymelgreen, T. Balli, T. Miloh, G. Yossifon, Active colloids as mobile microelectrodes for unified label-free selective cargo transport, *Nat. Commun.* 9 (2018), <https://doi.org/10.1038/s41467-018-03086-2>.
- [10] L. Wang, J. Chen, X. Feng, W. Zeng, R. Liu, Y. Xiujing Lin, L.W. Ma, Self-propelled manganese oxide-based catalytic micromotors for drug delivery, *RSC Adv.* 6 (2016) 65624–65630, <https://doi.org/10.1039/c6ra13739c>.
- [11] A.B. Pawar, I. Kretzschmar, Multifunctional patchy particles by glancing angle deposition, *Langmuir.* 25 (2009) 9057–9063, <https://doi.org/10.1021/la900809b>.
- [12] M. García, J. Orozco, M. Guix, W. Gao, S. Sattayasamitsathit, A. Escarpa, A. Merkoçi, J. Wang, Micromotor-based lab-on-chip immunoassays, *Nanoscale.* 5 (2016) 1325–1331, <https://doi.org/10.1039/c2nr32400h>.
- [13] A. Giacometti, F. Romano, F. Sciortino, Theoretical calculations of phase diagrams and self-assembly in patchy colloids, *RSC Smart Mater.* (2012) 108–137, <https://doi.org/10.1039/9781849735100-00108>.
- [14] G. Munaò, Z. Preisler, T. Vissers, F. Smallegang, F. Sciortino, Cluster formation in one-patch colloids: low coverage results, *Soft Matter.* 9 (2013) 2652–2661, <https://doi.org/10.1039/c2sm27490f>.
- [15] A. Kumar, B.J. Park, F. Tu, D. Lee, Amphiphilic Janus particles at fluid interfaces, *Soft Matter.* 9 (2013) 6604–6617, <https://doi.org/10.1039/c3sm50239b>.
- [16] Y. Lan, J. Choi, H. Li, Y. Jia, R. Huang, K.J. Stebe, D. Lee, Janus particles with varying configurations for emulsion stabilization, *Ind. Eng. Chem. Res.* 58 (2019) 20961–20968, <https://doi.org/10.1021/acs.iecr.9b02697>.
- [17] X. Wang, M. In, C. Blanc, A. Würger, M. Nobili, A. Stocco, Janus colloids actively rotating on the surface of water, *Langmuir.* 33 (2017) 13766–13773, <https://doi.org/10.1021/acs.langmuir.7b02353>.
- [18] W. Li, H. Palis, R. Merindol, J. Majimel, S. Ravaine, E. Duguet, Colloidal molecules and patchy particles: complementary concepts, synthesis and self-assembly, *Chem. Soc. Rev.* 49 (2020) 1955–1976, <https://doi.org/10.1039/x0xx00000x>.
- [19] G.R. Yi, D.J. Pine, S. Sacanna, Recent progress on patchy colloids and their self-assembly, *J. Phys. Condens. Matter.* 25 (2013), <https://doi.org/10.1088/0953-8984/25/19/193101>.
- [20] V. Meester, R.W. Verweij, C. Van Der Wel, D.J. Kraft, Colloidal recycling: reconfiguration of random aggregates into patchy particles, *ACS Nano.* 10 (2016) 4322–4329, <https://doi.org/10.1021/acsnano.5b07901>.
- [21] P. Sajeesh, A.K. Sen, Particle separation and sorting in microfluidic devices: a review, *Microfluid. Nanofluidics.* 17 (2014) 1–52, <https://doi.org/10.1007/s10404-013-1291-9>.
- [22] M. Lee, J. Bin Won, D.H. Jung, J. Kim, Y. Choi, K. Akyildiz, J. Choi, K. Kim, J. Cho, H. Yoon, H.-J. Koo, Dielectrophoretic manipulation of Janus particle in conductive media for biomedical applications, *Biotechnol. J.* (2020) 1–, <https://doi.org/10.1002/biot.202000343>.
- [23] B. Çetin, D. Li, Dielectrophoresis in microfluidics technology, *Electrophoresis.* 32 (2011) 2410–2427, <https://doi.org/10.1002/elps.201100167>.
- [24] J. Voldman, Electrical forces for microscale cell manipulation, *Annu. Rev. Biomed. Eng.* 8 (2006) 425–454, <https://doi.org/10.1146/annurev.bioeng.8.061505.095739>.
- [25] K. Zhao, D. Li, Numerical studies of manipulation and separation of Janus particles in nano-orifice based DC-dielectrophoretic microfluidic chips, *J. Micromechanics Microengineering.* 27 (2017), <https://doi.org/10.1088/1361-6439/aa7eae>.
- [26] K. Zhao, D. Li, Manipulation and separation of oil droplets by using asymmetric nano-orifice induced DC dielectrophoretic method, *J. Colloid Interface Sci.* 512 (2018) 389–397, <https://doi.org/10.1016/j.jcis.2017.10.073>.
- [27] K. Zhao, D. Li, Direct current dielectrophoretic manipulation of the ionic liquid droplets in water, *J. Chromatogr. A.* 1558 (2018) 96–106, <https://doi.org/10.1016/j.chroma.2018.05.020>.
- [28] C. Zhang, K. Khoshmanesh, A. Mitchell, K. Kalantar-Zadeh, Dielectrophoresis for manipulation of micro/nano particles in microfluidic systems, *Anal. Bioanal. Chem.* 396 (2010) 401–420, <https://doi.org/10.1007/s00216-009-2922-6>.
- [29] K. Khoshmanesh, S. Nahavandi, S. Baratchi, A. Mitchell, K. Kalantar-zadeh, Dielectrophoretic platforms for bio-microfluidic systems, *Biosens. Bioelectron.* 26 (2011) 1800–1814, <https://doi.org/10.1016/j.bios.2010.09.022>.
- [30] Y. Kang, B. Cetin, Z. Wu, D. Li, Continuous particle separation with localized AC-dielectrophoresis using embedded electrodes and an insulating hurdle, *Electrochim. Acta.* 54 (2009) 1715–1720, <https://doi.org/10.1016/j.electacta.2008.09.062>.
- [31] K. Zhao, D. Li, Continuous separation of nanoparticles by type via localized DC-dielectrophoresis using asymmetric nano-orifice in pressure-driven flow, *Sens. Actuat. B Chem.* 250 (2017) 274–284, <https://doi.org/10.1016/j.snb.2017.04.184>.
- [32] K. Zhao, R. Peng, D. Li, Separation of nanoparticles by a nano-orifice based DC-dielectrophoresis method in a pressure-driven flow, *Nanoscale.* 8 (2016) 18945–18955, <https://doi.org/10.1039/c6nr06952e>.
- [33] M.P. Hughes, Strategies for dielectrophoretic separation in laboratory-on-a-chip systems, *Electrophoresis* 23 (2002) 2569–2582, [https://doi.org/10.1002/1522-2683\(200208\)23:16<2569::AID-ELPS2569>3.0.CO;2-M](https://doi.org/10.1002/1522-2683(200208)23:16<2569::AID-ELPS2569>3.0.CO;2-M).
- [34] P.R.C. Gascoyne, J.V. Vykoukal, J.A. Schwartz, T.J. Anderson, D.M. Vykoukal, K. W. Current, C. McConaghy, F.F. Becker, C. Andrews, Dielectrophoresis-based programmable fluidic processors, *Lab Chip.* 4 (2004) 299–309, <https://doi.org/10.1039/b404130e>.
- [35] K. Zhao, Y. Wei, J. Dong, P. Zhao, Y. Wang, X. Pan, J. Wang, Separation and characterization of microplastic and nanoplastic particles in marine environment, *Environ. Pollut.* 297 (2022), <https://doi.org/10.1016/j.envpol.2021.118773>.
- [36] T.B. Jones, *Electromechanics of particles*, Cambridge University Press (1995), [https://doi.org/10.1016/S0032-5910\(97\)82724-6](https://doi.org/10.1016/S0032-5910(97)82724-6).
- [37] J. Chen, H. Zhang, X. Zheng, H. Cui, Janus particle microshuttle: 1D directional self-propulsion modulated by AC electrical field, *AIP Adv.* 4 (2014), <https://doi.org/10.1063/1.4868373> 031325.
- [38] P. Eppmann, B. Prügler, J. Gimsa, Particle characterization by AC electrokinetic phenomena 2. Dielectrophoresis of latex particles measured by dielectrophoretic phase analysis light scattering (DPALS), *Colloids Surfaces A Physicochem. Eng. Asp.* 149 (1999) 443–449, [https://doi.org/10.1016/S0927-7757\(98\)00304-5](https://doi.org/10.1016/S0927-7757(98)00304-5).
- [39] L. Zhang, Y. Zhu, Dielectrophoresis of Janus particles under high frequency ac-electric fields, *Appl. Phys. Lett.* 96 (2010), <https://doi.org/10.1063/1.3378687> 191605.
- [40] Hywel Morgan, Nicolas G Green, AC electrokinetics: Colloids and nanoplastics, *Encycl. Microfluid. Nanofluidics.* (2003) 8–8. https://doi.org/10.1007/978-0-387-48998-8_4.
- [41] V.N. Manoharan, M.T. Elsesser, D.J. Pine, Dense packing and symmetry in small clusters of microspheres, *Science (80-)* 301 (2003) 483–487, <https://doi.org/10.1029/2003GL016875>.
- [42] I. Ermolina, H. Morgan, The electrokinetic properties of latex particles: comparison of electrophoresis and dielectrophoresis, *J. Colloid Interface Sci.* 285 (2005) 419–428, <https://doi.org/10.1016/j.jcis.2004.11.003>.
- [43] P. García-Sánchez, Y. Ren, J.J. Arcenegui, H. Morgan, A. Ramos, Alternating current electrokinetic properties of gold-coated microspheres, *Langmuir.* 28 (2012) 13861–13870, <https://doi.org/10.1021/la302402v>.
- [44] A.B. Pawar, I. Kretzschmar, Patchy particles by glancing angle deposition, *Langmuir.* 24 (2008) 355–358, <https://doi.org/10.1021/la703005z>.
- [45] K. Dietrich, D. Renggli, M. Zanini, G. Volpe, I. Buttinoni, L. Isa, Two-dimensional nature of the active Brownian motion of catalytic microswimmers at solid and liquid interfaces, *New J. Phys.* 19 (2017), <https://doi.org/10.1088/1367-2630/aa7126>.
- [46] S. Ni, E. Marini, I. Buttinoni, H. Wolf, L. Isa, Hybrid colloidal microswimmers through sequential capillary assembly, *Soft Matter.* 13 (2017) 4252–4259, <https://doi.org/10.1039/c7sm00443e>.
- [47] S. Ni, J. Leemann, I. Buttinoni, L. Isa, H. Wolf, Programmable colloidal molecules from sequential capillarity-assisted particle assembly, *Sci. Adv.* 2 (2016) e1501779.
- [48] L. Alvarez, M.A. Fernandez-Rodríguez, A. Alegria, S. Arrese-Igor, K. Zhao, M. Kröger, L. Isa, Reconfigurable artificial microswimmers with internal feedback, *Nat. Commun.* 12 (2021) 4762, <https://doi.org/10.1038/s41467-021-25108-2>.
- [49] D.C. Duffy, J.C. McDonald, O.J.A. Schueller, G.M. Whitesides, Rapid prototyping of microfluidic systems in poly(dimethylsiloxane), *Anal. Chem.* 70 (1998) 4974–4984, <https://doi.org/10.1021/ac980656z>.
- [50] T. Honegger, O. Lecarme, K. Berton, D. Peyrade, 4-D dielectrophoretic handling of Janus particles in a microfluidic chip, *Microelectron. Eng.* 87 (2010) 756–759, <https://doi.org/10.1016/j.mee.2009.11.145>.
- [51] M. Li, D. Li, Separation of Janus droplets and oil droplets in microchannels by wall-induced dielectrophoresis, *J. Chromatogr. A.* 1501 (2017) 151–160, <https://doi.org/10.1016/j.chroma.2017.04.027>.
- [52] S. Gangwal, O.J. Cayre, O.D. Velev, Dielectrophoretic assembly of metallodielectric janus particles in AC electric fields, *Langmuir.* 24 (2008) 13312–13320, <https://doi.org/10.1021/la801522z>.
- [53] L. Zhang, Y. Zhu, Directed assembly of Janus particles under high frequency ac-electric fields: Effects of medium conductivity and colloidal surface chemistry, *Langmuir.* 28 (2012) 13201–13207, <https://doi.org/10.1021/la302725v>.

- [54] X.Y. Ling, I.Y. Phang, C. Acikgoz, M. Deniz Yilmaz, M.A. Hempenius, G. Julius Vancso, J. Huskens, Janus particles with controllable patchiness and their chemical functionalization and supramolecular assembly, *Angew. Chemie - Int. Ed.* 48 (2009) 7677–7682, <https://doi.org/10.1002/anie.200903579>.
- [55] F. Zhang, D. Li, Separation of dielectric Janus particles based on polarizability-dependent induced-charge electroosmotic flow, *J. Colloid Interface Sci.* 448 (2015) 297–305, <https://doi.org/10.1016/j.jcis.2015.02.006>.
- [56] K. Zhao, B.P. Larasati, D. Duncker, Li, Continuous cell characterization and separation by microfluidic alternating current dielectrophoresis, *Anal. Chem.* 91 (2019) 6304–6314, <https://doi.org/10.1021/acs.analchem.9b01104>.
- [57] K. Zhao, D. Li, Tunable droplet manipulation and characterization by ac-DEP, *ACS Appl. Mater. Interfaces.* 10 (2018) 36572–36581, <https://doi.org/10.1021/acsami.8b14430>.
- [58] W. Gao, J. Wang, The environmental impact of micro/nanomachines: a review, *ACS Nano.* 8 (2014) 3170–3180, <https://doi.org/10.1021/nn500077a>.
- [59] Y. Wu, R. Dong, Q. Zhang, B. Ren, Dye-enhanced self-electrophoretic propulsion of light-driven TiO₂-Au Janus micromotors, *Nano-Micro Lett.* 9 (2017) 30, <https://doi.org/10.1007/s40820-017-0133-9>.
- [60] J. Li, V.V. Singh, S. Sattayasamitsathit, J. Orozco, K. Kaufmann, R. Dong, W. Gao, B. Jurado-Sanchez, Y. Fedorak, J. Wang, Water-driven micromotors for rapid photocatalytic degradation of biological and chemical warfare agents, *ACS Nano.* 8 (2014) 11118–11125, <https://doi.org/10.1021/nn505029k>.
- [61] J.A.M. Delezuk, D.E. Ramírez-Herrera, B. Esteban-Fernández de Ávila, J. Wang, Chitosan-based water-propelled micromotors with strong antibacterial activity, *Nanoscale.* 9 (2017) 2195–2200, <https://doi.org/10.1039/c6nr09799e>.
- [62] Y. Ge, M. Liu, L. Liu, Y. Sun, H. Zhang, B. Dong, Dual-fuel-driven bactericidal micromotor, *Nano-Micro Lett.* 8 (2016) 157–164, <https://doi.org/10.1007/s40820-015-0071-3>.
- [63] J. Orozco, L.A. Mercante, R. Pol, A. Merkoçi, Graphene-based Janus micromotors for the dynamic removal of pollutants, *J. Mater. Chem. A.* 4 (2016) 3371–3378, <https://doi.org/10.1039/c5ta09850e>.
- [64] C.E. Sing, L. Schmid, M.F. Schneider, T. Franke, A. Alexander-Katz, Controlled surface-induced flows from the motion of self-assembled colloidal walkers, *Proc. Natl. Acad. Sci.* 107 (2010) 535–540, <https://doi.org/10.1073/pnas.0906489107>.
- [65] M. Driscoll, B. Delmotte, M. Youssef, S. Sacanna, A. Donev, P. Chaikin, Unstable fronts and motile structures formed by microrollers, *Nat. Phys.* 13 (2017) 375–379, <https://doi.org/10.1038/nphys3970>.
- [66] D. Geyer, A. Morin, D. Bartolo, Sounds and hydrodynamics of polar active fluids, *Nat. Mater.* 17 (2018) 789–793, <https://doi.org/10.1038/s41563-018-0123-4>.
- [67] B. Jurado-Sánchez, S. Sattayasamitsathit, W. Gao, L. Santos, Y. Fedorak, V.V. Singh, J. Orozco, M. Galarnyk, J. Wang, Self-propelled activated carbon Janus micromotors for efficient water purification, *Small.* 11 (2015) 499–506, <https://doi.org/10.1002/smll.201402215>.
- [68] M. Xuan, X. Lin, J. Shao, L. Dai, Q. He, Motion-based, high-yielding, and fast separation of different charged organics in water, *ChemPhysChem.* 16 (2015) 147–151, <https://doi.org/10.1002/cphc.201402795>.
- [69] M. Youssef, T. Hueckel, G.R. Yi, S. Sacanna, Shape-shifting colloids via stimulated dewetting, *Nat. Commun.* 7 (2016) 1–7, <https://doi.org/10.1038/ncomms12216>.
- [70] Z. Gong, T. Hueckel, G.R. Yi, S. Sacanna, Patchy particles made by colloidal fusion, *Nature.* 550 (2017) 234–238, <https://doi.org/10.1038/nature23901>.
- [71] P.J.M. Swinkels, S.G. Stuij, Z. Gong, H. Jonas, N. Ruffino, B. van der Linden, P.G. Bolhuis, S. Sacanna, S. Woutersen, P. Schall, Revealing pseudorotation and ring-opening reactions in colloidal organic molecules, *Nat. Commun.* 12 (2021), <https://doi.org/10.1038/s41467-021-23144-6>.
- [72] Z. Wang, Z. Wang, J. Li, S.T.H. Cheung, C. Tian, S.H. Kim, G.R. Yi, E. Ducrot, Y. Wang, Active patchy colloids with shape-tunable dynamics, *J. Am. Chem. Soc.* 141 (2019) 14853–14863, <https://doi.org/10.1021/jacs.9b07785>.
- [73] Z. Nie, W. Li, M. Seo, S. Xu, E. Kumacheva, Janus and ternary particles generated by microfluidic synthesis: design, synthesis, and self-assembly, *J. Am. Chem. Soc.* 128 (2006) 9408–9412, <https://doi.org/10.1021/ja060882n>.
- [74] R. Pioli, M.A. Fernandez-Rodriguez, F. Grillo, L. Alvarez, R. Stocker, L. Isa, E. Secchi, Sequential capillarity-assisted particle assembly in a microfluidic channel, *Lab Chip.* 21 (2021) 888–895, <https://doi.org/10.1039/d0lc00962h>.